Phase diagrams of Pb-free solders and their related materials systems

Sinn-Wen Chen · Chao-Hong Wang · Shih-Kang Lin · Chen-Nan Chiu

Published online: 1 September 2006

Abstract Replacing Pb–Sn with Pb-free solders is one of the most important issues in the electronic industry. Melting, dissolution, solidification and interfacial reactions are encountered in the soldering processes. Phase diagrams contain equilibrium phase information and are important for the understanding and prediction of phase transformation and reactive phase formation at the solder joints. This study reviews the available phase diagrams of the promising Pb-free solders, and their related materials systems. The solders are Sn–Ag, Sn–Cu, Sn–Ag–Cu, Sn–Zn, Sn–Bi, Sn–In and Sn–Sb. The materials systems are the solders with the Ag, Au, Cu, Ni substrates, such as Sn–Ag–Au, Sn–Ag–Ni, Sn–Cu–Au, and Sn–Cu–Ni ternary systems. For the Pb-free solders and their related ternary and quaternary systems, preliminary phase equilibria information is available; however, complete and reliable phase diagrams over the entire compositional and temperature ranges of soldering interests are lacking.

1 Introduction

Soldering is the most important joining technology in the electronic industries [1]. Solders are heated up and melt first during the soldering processes. The molten solders wet the substrates, and liquid (solder)/solid (substrate) contacts are formed. The joints are then cooled down, solders solidify, and solder joints are formed. Since melting is required in the soldering processes, solders are usually low melting point alloys. Pb–Sn alloys are the most popular solders and their properties are extensively investigated. However, due to health and environmental concerns, the European Union has made resolution prohibiting Pb usage in the electronic products [2], and the electronic industries are now shifting to Pb-free solders [3–5].

Soldering is conducted at the completely molten state of solders, while the solder products are in use with the solders at their solid phases. The primary materials characteristics of solders are their liquidus and solidus temperatures which define the temperature boundaries of completely molten and completely solid, respectively. Solders melt and wet the substrates at temperatures higher than their melting points, and there are dissolution of substrates and interfacial reactions between solders and substrates [1, 4–6]. The liquid phase then transforms to various solid phases when the joints are cooled down. The different kinds and relative amounts of the solid phases formed during solidification are important for the solder joint properties.

Since solders are low melting point alloys, the products' operation temperatures are relatively high temperatures and diffusion is significant for most solders. In addition, good wetting is required for good solders, thus interfacial reactions with substrates are usually significant not only at the liquid/solid contacts, but at the solid/solid contacts at the operation temperatures as well. Interfacial reactions at the solder joints are the key reliability factor of electronic products. Understanding and controlling of the interfacial reactions are important, because the interfacial

S.-W. Chen (✉) · C.-H. Wang · S.-K. Lin · C.-N. Chiu
Department of Chemical Engineering, National Tsing Hua University, Hsin-chu, Taiwan
e-mail: swchen@che.nthu.edu.tw

reactions are more complicated with Pb-free solders and with the emerging flip chip technologies which are with more pronounced electromigration effects.

Solders are usually binary and ternary alloys. When they are in contact with substrates, the materials systems are then ternary, quaternary or even of higher orders. As mentioned above, phase transformation and reactive phase transformation occurs at the solder joints. Phase diagrams contain the basic phase equilibria and phase transformation information, such as the solidus and liquidus temperatures of alloys. Besides, the liquidus projection can be used for the illustration of solidification path. Isothermal section is crucial for the understanding of interfacial reactions. Phase diagrams of Pb-free solders and their related materials systems are important for the applications of Pb-free solders.

Among various kinds of Pb-free solders, Sn–Ag, Sn–Cu, Sn–Ag–Cu, Sn–Zn-(based), Sn–Bi, Sn–In and Sn–Sb alloys are most promising. Ag, Au, Cu and Ni are the most common substrates. This study reviews the research status of the phase diagrams of these promising solders and the materials systems including solders and substrates, such as Sn–Ag–Au, Sn–Ag–Ni, Sn–Cu–Au and Sn–Cu–Ni. Since interfacial reactions are important for soldering applications, and they also provide the phase formation information, interfacial reactions literatures related directly with phase formations are also included in this study, especially for the materials system with no available phase equilibria information.

2 Sn–Ag–Cu (Sn–Ag and Sn–Cu)

Eutectic and near eutectic Sn–Ag–Cu (SAC) alloys are recommended by JEIDA and NEMI [7, 8]. Sn–0.7wt%Cu (Sn–1.3at%Cu) and Sn–3.5wt%Ag (Sn–3.8at%Ag) are also promising Pb-free solders. The most important Pb-free solders are at the Sn-rich corner of the Sn–Ag–Cu ternary system composed of the binary Sn–Cu eutectic, binary Sn–Ag eutectic and the ternary Sn–Ag–Cu eutectic.

As shown in Fig. 1 [9] of the Sn–Ag binary system, there are two intermetallic compounds, ζ-Ag_4Sn and ε-Ag_3Sn, two peritectic reactions, and one eutectic reaction, liquid = Ag_3Sn + Sn [9]. The eutectic composition is at Sn–3.5wt%Ag and its melting temperature is at 221°C. Kattner and Boettinger [10] have thermodynamically modeled this system. They used solution models for Ag, Sn, liquid, and the ζ phase, and they assumed the ε-Ag_3Sn to be a line compound. The calculated phase diagrams are in good agreement with the experimental determinations, and the temperature and liquid composition of the eutectic are at 220.9°C and Sn–3.87at%Ag, respectively.

The binary Sn–Cu system is a complicated binary system. As shown in Fig. 2, there are seven intermetallic compounds (β, γ, ζ, δ, ε-Cu_3Sn, η-Cu_6Sn_5 and η'-Cu_6Sn_5), and 13 invariant reactions [11]. For soldering application purposes, phase equilibria at the Sn-rich corner are more important, and there are 3 intermetallic compounds, ε-Cu_3Sn, η-Cu_6Sn_5 and η'-Cu_6Sn_5, one eutectic, liquid = Sn + η – Cu_6Sn_5, and one possible eutectoid, η-Cu_6Sn_5 = Sn + η' – Cu_6Sn_5. The liquid composition and the temperature of the eutectic are at Sn–0.7wt%Cu and 227°C. Shim et al. [12] and Boettinger et al. [13] have thermodynamically modeled the binary Sn–Cu system. The ζ, δ, ε-Cu_3Sn, η-Cu_6Sn_5 and η'-Cu_6Sn_5 are assumed to be line compounds. Solution model and two-sublattices model are used for the β and γ phases, respectively. The calculated phase diagrams are in good agreement with the experimental determinations.

Gebhardt and Petzow [14] and Yen and Chen [15] experimentally determined the isothermal sections of the phase equilibria of the ternary Sn–Ag–Cu system. No ternary compounds have been found. As shown in Fig. 3a of the 240°C isothermal section, the ε-Cu_3Sn phase has tie-lines with all the solid phases, and the ternary solubilities of the binary compounds are limited. Gebhardt and Petzow [14] proposed a class II reaction, L + η-Cu_6Sn_5 = ε-Ag_3Sn + Sn, at the Sn-rich corner at 225°C. The experimental results of Miller et al. [16] indicated a different result and the invariant reaction should be a class I reaction L = η-Cu_6Sn_5 + ε-Ag_3Sn + Sn at 216.8°C. The Sn–Ag–Cu liquidus projection is shown in Fig. 3b. More recent phase equilibria studies all agree that the invariant reaction at the Sn-rich corner is a class I reaction [15, 17–19]. However, the exact composition and temperature of the class I reaction, the ternary eutectic varied. Loomans and Fine [17] reported the eutectic composition to be at Sn–3.5wt%Ag–0.9wt%Cu (Sn–3.81at%Ag–1.66at%Cu). The liquid composition and temperature of the ternary eutectic determined by Moon et al. [18] are Sn–3.5wt%Ag–0.9wt%Cu and 217.2°C, and are Sn–3.66wt%Ag–0.91wt%Cu (Sn–3.98at%Ag–1.68at%Cu) and 216.3°C from their calculation. The ternary eutectic is at Sn–3.24wt%Ag-0.57wt%Cu and 217.7°C as determined by Ohnuma et al. [19].

The materials systems consisting of the solders and popular substrates, Au, Ag, Cu, Ni, are important for soldering applications as well. Massalski and Pops [20] and Evans and Prince [21] experimentally determined the phase equilibria of the Sn–Ag–Au ternary system.

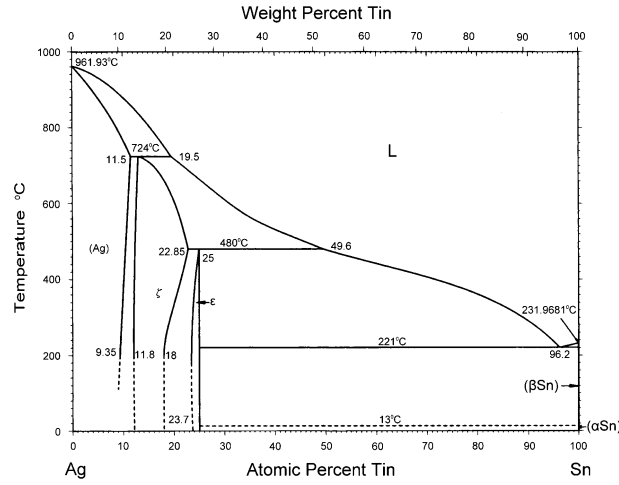

Fig. 1 The Sn–Ag binary phase diagram [9]

Figure 4a is the phase equilibria isothermal section of the ternary Sn–Ag–Au system at 200°C proposed based on phase equilibria and interfacial reaction results [20–22]. No ternary compounds have been found. Continuous solid solutions are formed between Ag and Au, and the ζ phase in the Au–Sn and Ag–Sn systems. The ε-Ag_3Sn phase has about 10at% Au solubility, while the ternary solubilities of other Au–Sn binary compounds are negligible. Figure 4b is the liquidus projection of the Sn–Ag–Au system [21]. At the Sn-rich corner, there is class I reaction, ternary eutectic liquid = ε-Ag_3Sn + Sn + η-$AuSn_4$, at 206°C. Chen and Yen [22] examined the interfacial reactions in the Ag–Sn/Au couples. Three binary phases, δ-AuSn, ε-$AuSn_2$, and η-$AuSn_4$, were formed in all the couples. The results are in agreement with the phase diagrams studies that all the compounds do not have detectable ternary solubility.

Interfacial reactions between Sn–3.5wt%Ag and Cu substrates have been studied by various groups [23–27]. In agreement with the Sn–Ag–Cu phase diagrams [15, 17–19], no ternary compound is formed, and the reaction products are binary ε-Cu_3Sn and η-Cu_6Sn_5 phase in the temperature range between 70°C and 360°C. It needs mentioning that although an order-disorder transformation of the Cu_6Sn_5 phase reaction is observed [11–13], the effect of this transformation has not been discussed in either the ternary phase

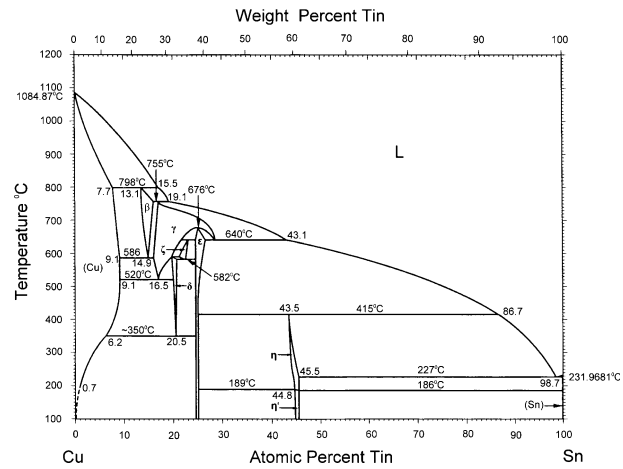

Fig. 2 The Sn–Cu binary phase diagram [11]

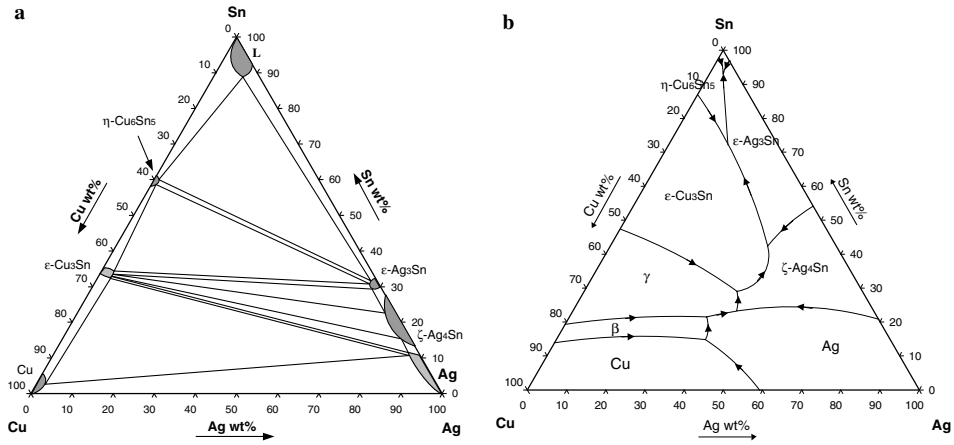

Fig. 3 (**a**) The 240°C isothermal section of the Sn–Ag–Cu ternary system [15]. (**b**) Liquidus projection of the Sn–Ag–Cu ternary system [14]

equilibria studies [14–19] or in the interfacial reaction studies [23–27].

Hsu and Chen [28] and Chen et al. [29] experimentally determined the isothermal sections and liquidus projections of the Sn–Ag–Ni ternary system. The phase diagrams of the ternary system were also calculated using the binary thermodynamic models without introducing any ternary interaction parameters [28]. Figure 5a, b are the 240°C isothermal section and the liquidus projection of the Sn–Ag–Ni ternary system, respectively. No ternary compounds have been found. The Ni_3Sn_2 phase is a very stable phase, and is in equilibrium with Ag, ζ-Ag_4Sn, ε-Ag_3Sn, Ni_3Sn, and Ni_3Sn_4 phases. It is also observed that all the ternary solubilities of the binary compounds are negligible. The liquid miscibility gap in the Ag–Ni binary system extends into the ternary system as shown in Fig. 8 of the liquidus projection. It is also shown in Fig. 5b that the class I reaction, ternary eutectic liquid = Sn + Ag_3Sn + Ni_3Sn_4, exists at the Sn-rich corner at 212.3°C. The interfacial reactions between Sn–3.5wt%Ag and Ni have been examined [28, 30–32]. In agreement with the phase diagram study [28], no ternary compound is formed in the Sn–Ag/Ni couples,

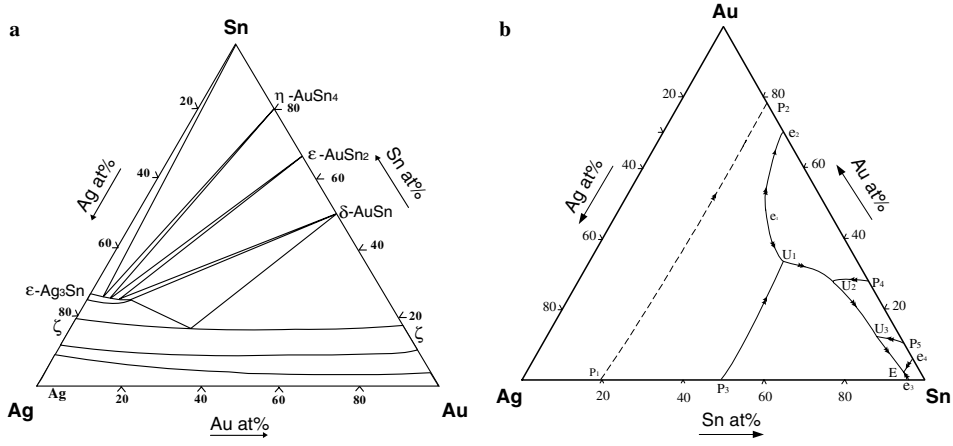

Fig. 4 (**a**) The 200°C isothermal section of the Sn–Ag–Au ternary system [22]. (**b**) Liquidus projection of the Sn–Ag–Au ternary system [21]

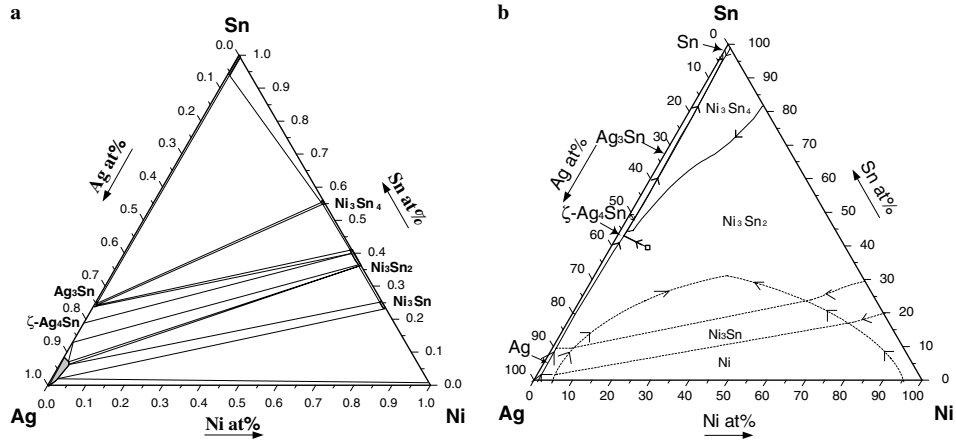

Fig. 5 (**a**) The 240°C isothermal section of the Sn–Ag–Ni ternary system [28]. (**b**) Liquidus projection of the Sn–Ag–Ni ternary system [29]

and Ni_3Sn_4 phase is the primary interfacial reaction product with negligible Ag solubility. Interfacial reactions with Ni are frequently examined because Ni is a popular substrate. However, it is worthy noting that Ni(P) and Ni–7wt%V substrates are often used in the electronic products besides pure Ni, and it has been found the interfacial reactions at the solder/Ni and solder/Ni–7wt%V are different [33].

The 360°C isothermal section of the Sn–Cu–Au phase diagram was determined by Karlsen et al. [34] as shown in Fig. 6. Continuous solid solutions are formed between Cu and Au and between the δ-AuSn and η-Cu_6Sn_5 phases. Three ternary intermetallic compounds, designated as A, B, and C, were found. The compositional ranges are $Sn_{20}Cu_{38}Au_{42}$–$Sn_{20}Cu_{33}Au_{47}$, $Sn_{20}Cu_{69}Au_{11}$–$Sn_{20}Cu_{42}Au_{38}$, and $Sn_{333}Cu_{337}Au_{330}$–$Sn_{333}Cu_{297}Au_{370}$, respectively. It can be noticed that all the homogeneity ranges of the binary compounds and the ternary compounds are all in the directions parallel to Au–Cu side, indicating the Au and Cu atoms are easier to interchange atomic sites with each other. Peplinski and Zakel [35] investigated the Sn–Cu–Au alloys by X-ray powder diffraction, and they reported the existence of a ternary compound $Sn_4Cu_8Au_8$ with compositional ranging from $Sn_4Cu_9Au_7$ to $Sn_4Cu_7Au_9$. This phase is in agreement with the A phase reported by Karlsen et al. [34]. Luciano et al. [36] studied the pseudobinary phase diagram, and they found the B phase, a ternary compound, in the results by Karlsen et al. is the ordered AuCu III' phase. Although Au surface is frequently encountered in electronic products, and the formation of the $AuSn_4$ phase causes various problems [37], no interfacial reactions studies of the Sn–Cu alloy with pure Au substrate are available.

Lin et al. [38], Wang and Chen [39] and Chen et al. [40] experimentally determined the phase equilibria of the Sn–Cu–Ni ternary system. Figure 7a is the 240°C Sn–Cu–Ni phase equilibria isothermal section. No ternary compounds have been found. Cu and Ni form a continuous (Cu,Ni) solid solution, and Cu_3Sn and Ni_3Sn formed a continuous $(Cu,Ni)_3Sn$ solid solution [38]. It is very distinguishable in the Sn–Cu–Ni system that the binary compounds are with very extensive solubility, but only along the direction parallel to the Cu–Ni side. However, Murakami and Kachi [41] reported a phase

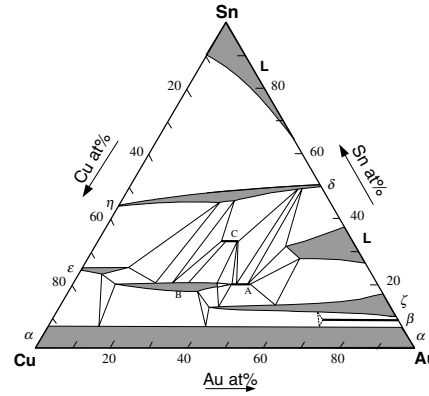

Fig. 6 The 360°C isothermal section of the Sn–Cu–Au ternary system [34]

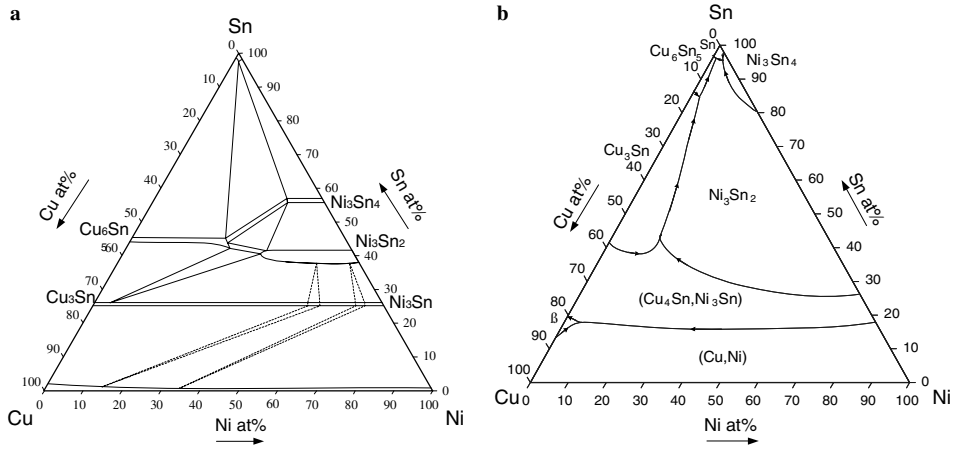

Fig. 7 (**a**) The 240°C isothermal section of the Sn–Cu–Ni ternary system [38]. (**b**) Liquidus projection of the Sn–Cu–Ni ternary system [38]

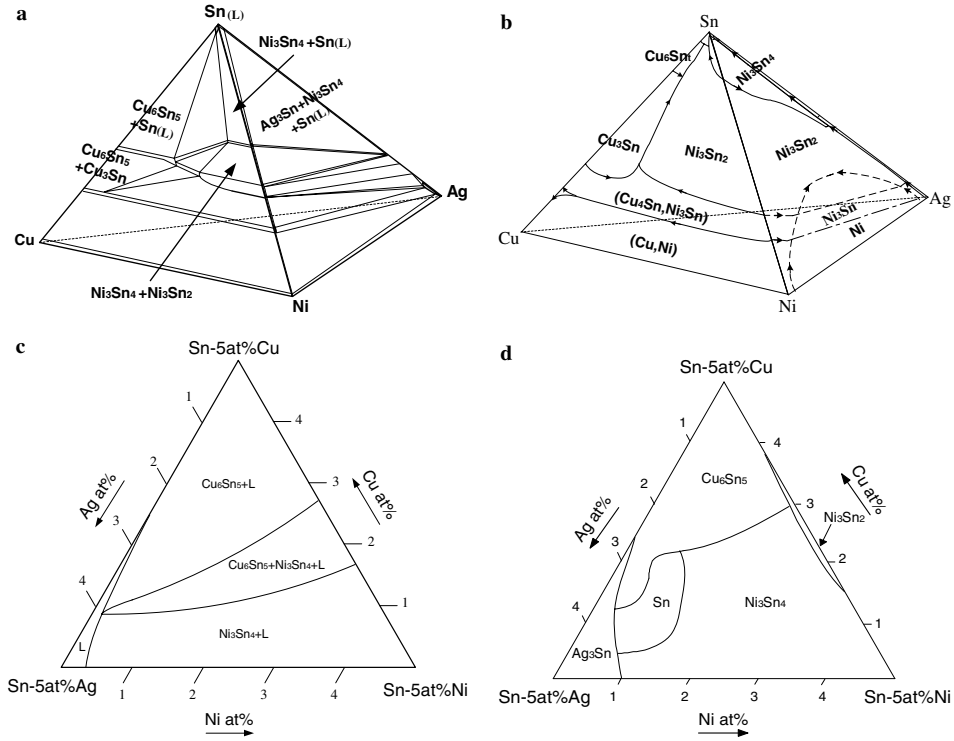

Fig. 8 (**a**) The 250°C isothermal tetrahedron of the Sn–Ag–Cu–Ni system [48]. (**b**) Liquidus projection tetrahedron of the Sn–Ag–Cu–Ni system [49]. (**c**) The 95at%Sn isoplethal section of the 250°C isothermal phase equilibria tetrahedron of the Sn–Ag–Cu–Ni system [50]. (**d**) The 95 at%Sn isoplethal section of the liquidus projection of the Sn–Ag–Cu–Ni system [49]

transformation of this $(Cu,Ni)_3Sn$ solid solution. A continuous solid solution cannot exist if there is a phase transformation. Lin et al. [38] marked dashed lines on the 240°C phase diagrams regarding the inconsistency. Oberndorff determined the isothermal section at 235°C [42], and they reported the formation of a ternary compound with an average composition $Sn_{44}Cu_{27}Ni_{29}$. Fig. 7b is the liquidus projection of the Sn–Cu–Ni system. At the Sn-rich corner which is of primary soldering interests, there is a class I reaction, a ternary eutectic liquid = Sn + Ni_3Sn_2 + Cu_6Sn_5 and a class II reaction, liquid + Ni_3Sn_4 = Sn + Ni_3Sn_2.

Miettinen [43] is the only work that has thermodynamically modeled the Sn–Cu–Ni system but only at the Cu–Ni side. A good description of the thermodynamic models at the Sn-rich corner which is interesting to the soldering application is still lacking. The interfacial reactions between Sn–Cu/Ni have been examined by various investigators [40, 44–47]. No ternary compounds have been observed. It is found that the interfacial products are sensitive to Cu contents. When the Cu is less than 0.4 wt%, Ni_3Sn_4 phase formed, and the product is the Cu_6Sn_5 phase when the Cu content is higher. A peculiar interfacial reaction phenomenon has been observed in the Cu/Sn/Ni type couples [40], and the Cu_6Sn_5 phase is formed on both sides of the Sn solder. As shown in Fig. 7a, the Cu_6Sn_5 phase has very wide compositional homogeneity ranges, and thus the Cu_6Sn_5 phase can be stabilized with addition of Ni. The very significant Ni and Cu mutual solubilities in the Cu_6Sn_5 phase and the Ni_3Sn_4 phase result in complicated cross effects, and is the primary reason for the complicated interfacial reactions in the Sn–Cu/Ni couples. It is worth mentioning that owing to the very large mutual solubilities, some researchers use $(Cu,Ni)_6Sn_5$ and $(Cu,Ni)_3Sn_4$ for the Cu_6Sn_5 and Ni_3Sn_4 phases.

Chen et al. [48–50] determined the phase relationship of Sn–Ag–Cu–Ni ternary system. A tetrahedron is used for the description of the isothermal phase equilibria and for the liquidus projection as shown in Fig. 8a, b. No ternary and quaternary compounds have been found. Figure 8c,d are the 95at%Sn isoplethal sections of the 250°C phase equilibria and the liquidus projection, respectively. Since the Cu_6Sn_5 phase and the Ni_3Sn_4 phases contain negligible Ag, while the Ag_3Sn phase contains negligible Cu and Ni, the Cu_6Sn_5–Ni_3Sn_4edge of the four-phase tetrahedron is very close to the Sn–Cu–Ni side of the Sn–Ag–Cu–Ni tetrahedron, and the Ag_3Sn corner is nearly on the Sn–Ag–Ni side. The compositional phase regimes consisting Ag phases are very small which indicates the phase relationship in most compositional part is similar to that of Sn–Cu–Ni.

Various investigators have studied the Sn–Ag–Cu/Ni interfacial reactions [51–55]. In agreement with the phase diagram studies, the interfacial reactions are similar to those in the Sn–Cu/Ni couples [40, 44–47], and the Ag does not actively participate in the interfacial reactions. The reaction products are sensitive to Cu contents, and are either Cu_6Sn_5 or Ni_3Sn_4 phases. Since Sn–Ag–Cu alloy is the most promising Pb-free solder, phase diagram of the quaternary Sn–Ag–Cu–Ni system is important for Pb-free soldering. For the higher order materials systems, it is very difficult and not practical to experimentally determine the phase diagram through the whole temperature and compositional ranges. The CALPHAD (CALculation of PHAse Diagrams) [56] approach combines thermochemistry and phase equilibria. With the CALPHAD approach, the phase diagram of the quaternary Sn–Ag–Cu–Ni system can be calculated with the thermodynamic models of their constituent ternary systems and possible interaction parameters. The interaction parameters can be determined with limited experimental quaternary results [48–50]. Thermodynamic models for the Sn–Ag–Cu, Sn–Ag–Ni, and Ag–Cu–Ni are available [18, 19, 28, 57], and the only important part that is missing is a good thermodynamic description of the Sn–Cu–Ni ternary system.

3 Sn–Zn

Although Sn–Ag–Cu alloys are the most promising Pb-free solders, their melting points are much higher than that of the conventional Pb–Sn eutectic which is at 183°C. Various efforts have been carried out to develop Pb-free solders of more suitable melting points. The melting point of Sn–Zn eutectic alloy is at 198.5°C [58] and is closer to that of the eutectic Pb–Sn. Besides, Sn–Zn eutectic has good mechanical properties and low cost, and is likely a good candidate [59–66]. It has been recognized that poor wetting properties and serious oxidation problems are the obstacles for industrial applications of the pure binary Sn–Zn eutectic alloys. Improvements are achieved with introducing alloying elements and the results indicate the Sn–Zn-based alloys are promising low melting point solders [60, 63, 66].

As shown in Fig. 9, the binary Sn–Zn system is a simple eutectic system. The eutectic is at 198.5°C and Sn–8.8wt%Zn (Sn–14.9at%Zn), and the mutual solubilities of Sn and Zn are negligible [58]. Thermodynamic assessments of the Sn–Zn binary system and phase diagrams are calculated by Lee [67] and Ohtani et al. [68]. The results by Lee [67] are satisfactory, and

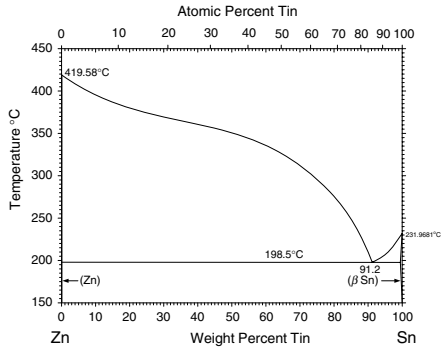

Fig. 9 The Sn–Zn binary phase diagram [58]

the calculated eutectic is at 198.25°C and Sn–14.8at%Zn.

Ohtani et al. [68] carried out thermal analysis and experimental phase equilibria studies of the Sn–Zn–Ag ternary system. They also developed thermodynamic models and calculated the isothermal sections at 420 and 190°C and the liquidus projection. Figure 10a is the 190°C isothermal section calculated by Ohtani et al. [68]. No ternary compounds have been found, and ternary solubilities of all the binary compounds are very limited. The calculated Sn-rich corner of the Sn–Zn–Ag liquidus projection is shown in Fig. 10b. The calculated ternary invariant reaction of the lowest reaction temperature is a class II reaction, liquid + ε-$AgZn_3$ = Sn + Zn, at 193.7°C. However, the binary Sn–Zn eutectic temperature calculated by Ohtani et al. [68] is at 181°C (as label on the figure, or at 191°C as read directly from the figure) and is too low comparing to the experimental value. The class II invariant reaction might be a class I reaction if the binary eutectic liquid = Sn + Zn is at 198.5°C. No interfacial reaction studies between Sn–Zn alloys and Ag substrate are available. Song and Lin [63] studied the solidification behavior of the Sn–8.87wt%Zn–1.5wt%Ag (Sn–14.99at%Zn–1.53at%Ag) alloy. They have found the existence of γ-Ag_5Zn_8 and ε-$AgZn_3$, and they also conclude that the intermetallic compound solidified first. These observations are in agreement with sequence predicted from the liquidus projection. However, the reaction temperatures are different. More experimental efforts and thermodynamic re-assessment are needed for the Sn–Zn–Ag system.

No phase diagram is available for the Sn–Zn–Au ternary system. Binary Au–Zn compounds are found from the interfacial reactions between Sn–Zn solder and Au finish [64, 65], and to date no ternary Sn–Zn–Au compounds are reported. Lee et al. calculated the phase diagram of Sn–Zn–Cu [69] with very limited experimental results. Chou and Chen [70] experimentally determined the isothermal sections of phase equilibria at 210, 230 and 250°C. Figure 11 is the Sn–Zn–Cu 230°C isothermal section. No ternary compounds have been found. However, in contrast to the calculated results [69], the experimental results indicate that Sn phase has tie-lines with the η-Cu_6Sn_5 phase and all the binary Cu–Zn compounds at 230 and 250°C. Thermodynamic re-assessment of the Sn–Zn–Cu ternary system is needed, so that accurate phase diagrams

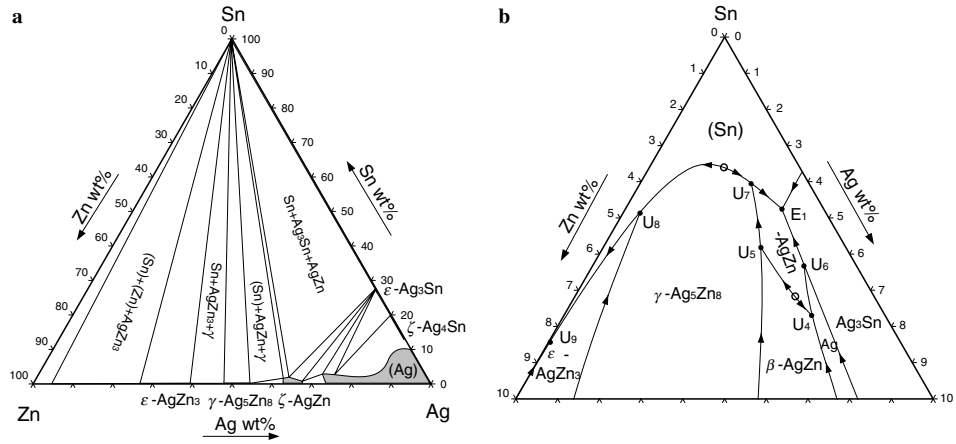

Fig. 10 (**a**) The 190°C isothermal section of the Sn–Zn–Ag ternary system [68]. (**b**) Liquidus projection of the Sn–Zn–Ag ternary system at the Sn-rich corner [68]

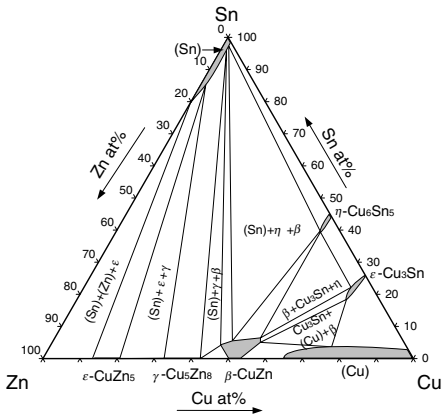

Fig. 11 The 230°C isothermal section of the Sn–Zn–Cu ternary system [70]

can be calculated. Various groups have studied the interfacial reactions Sn–Zn alloys reactions with Cu substrate [59, 61, 62, 64–66, 71]. Even though the Zn content is only 9 wt%, the interfacial reactions products are the Cu–Zn binary compounds with γ-Cu_5Zn_8 is the most dominating reaction phase.

No phase diagrams are available for the Sn–Zn–Ni ternary system. γ-Ni_5Zn_{21} compound is the primary interfacial reaction products in the Sn–Zn/Ni couples substrates [61, 64–66, 71]. However, with 41 h reaction at 280°C, besides the γ-Ni_5Zn_{21} phase, a layer of Sn–30.9at%Ni–16.3at%Zn composition is formed and it is likely to be the δ-Ni_3Sn_4 phase with 16.3 at%Zn [71]. A similar double layer formation is found in the Sn–8wt%Zn–3wt%Bi/Ni couple reacted at 325°C, and besides the γ-Ni_5Zn_{21} phase, a layer of Sn–35at%Ni–22at%Zn is formed [72]. Phase diagram study of the Sn–Zn–Ni system is needed to verify whether the compound is a thermodynamically stable or meta-stable phase and whether it is a binary or ternary compound.

4 Sn–Bi

Sn–Bi alloy is another low melting-point Pb-free solder. As shown Fig. 12, similar to the Sn–Pb system, the binary Sn–Bi system is a simple eutectic system without any intermetallic compound [10, 73, 74]. The eutectic is at 139°C and Sn–57wt%Bi (Sn–42.95at%Bi). Kattner and Boettinger [10] and Lee et al. [74] have developed thermodynamic models to calculate the Sn–Bi phase diagram, and the calculated results are in good agreement with the experimental determinations.

Various groups have determined the phase diagrams of the the Sn–Bi–Ag system [10, 75, 76]. No ternary compounds have been found, and all the binary compounds have negligible ternary solubilities. Figure 13a, b are the 230°C phase equilibria isothermal section and liquidus projection, respectively [10]. The liquidus projections obtained by three groups most recently [10, 75, 76] are similar. All of the results suggest there are one class I reaction, liquid = Sn + Bi+ε-Ag_3Sn, and two class II reactions. The temperatures of the class I reaction determined by the three groups are similar as well, and are 136.5, 138.4 and 139.2°C, by Kattner and Boettinger [10], Hassam et al. [75] and Ohtani et al. [76], respectively. However, the temperatures of the class II reaction, liquid+ζ = ε-Ag_3Sn + Bi, are very different at 238.6, 261.8, and 262.5°C, respectively.

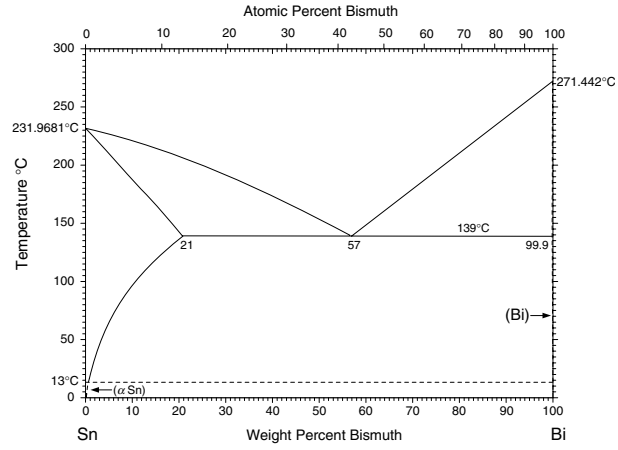

Fig. 12 The Sn–Bi binary phase diagram [73]

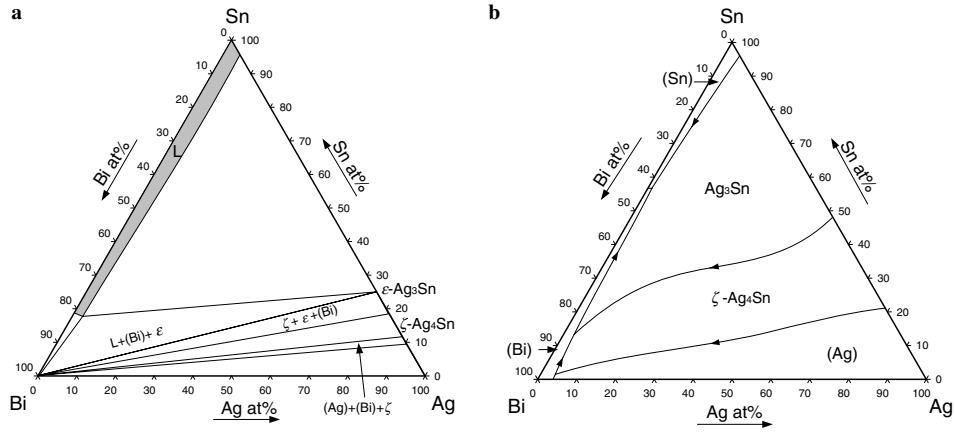

Fig. 13 (**a**) The 230°C isothermal section of the Sn–Bi–Ag ternary system [10]. (**b**) Liquidus projection of the Sn–Bi–Ag ternary system [10]

Partial isothermal sections of the Sn–Bi–Au ternary system at 139, 160, 200 and 240°C and the liquidus projection at the Sn-rich corner in the Sn–Bi–AuSn compositional regime have been determined [77]. As shown in Fig. 14a of the 200°C isothermal section, no ternary compounds have been found in this temperature and composition regime. The Bi solubility in the binary compounds, AuSn, $AuSn_2$ and $AuSn_4$ are negligible. Figure 14b is the partial liquidus projection, and there is a class I reaction, liquid = Sn + Bi + $AuSn_4$, at the Sn-rich corner. Interfacial reactions between Sn–Bi and Au are examined in a new fluxless bonding process in air using Sn–Bi with Au cap [78]. In agreement with the phase diagrams, the intermetallic compounds are Au–Sn binary compounds with almost no detectable Bi [78].

Lee et al. [69] calculated the phase diagrams of the Sn–Bi–Cu ternary system with the thermodynamic models developed from extension of those of the constituent binary systems without ternary interaction parameter. Doi et al. [79] experimentally examined the phase boundaries with DSC and developed thermodynamic models with a ternary interaction parameter of the liquid phase for the Sn–Bi–Cu system. No ternary compounds are found, and all the binary compounds are with negligible solubility [79]. Figure 15a, b

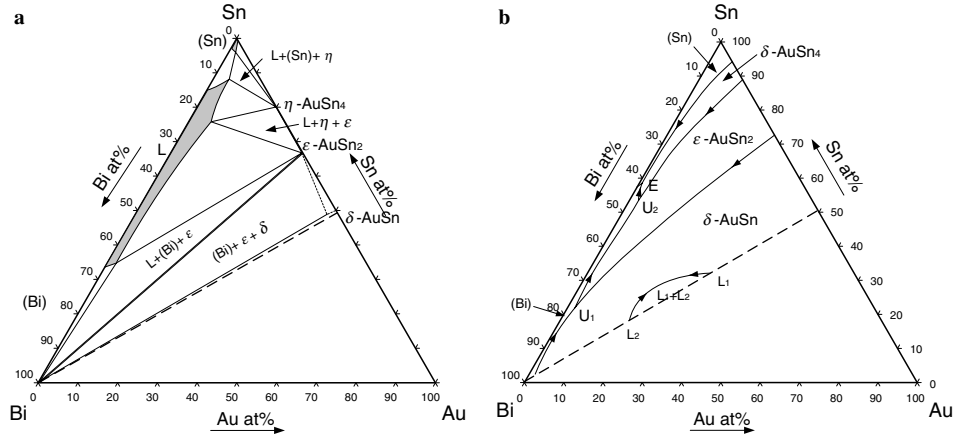

Fig. 14 (**a**) A partial 200°C isothermal section of the Sn–Bi–Au ternary system [77]. (**b**) A partial liquidus projection of the Sn–Bi–Au ternary system [77]

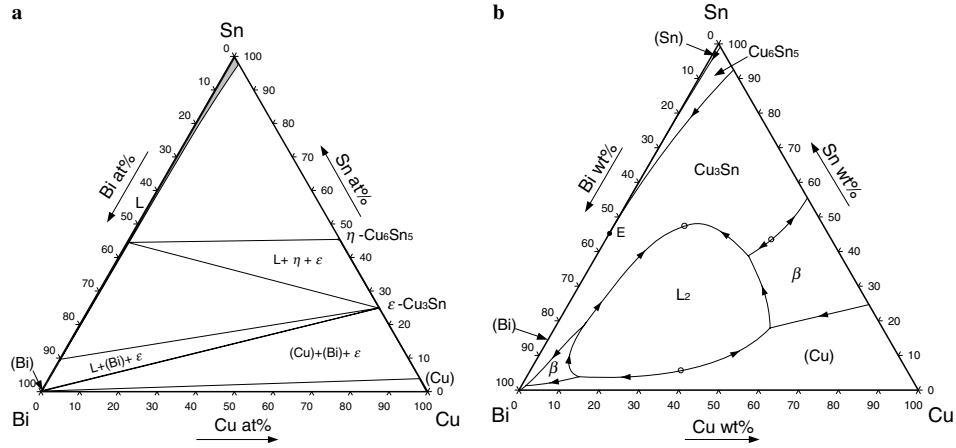

Fig. 15 (**a**) The 250°C isothermal section of the Sn–Bi–Cu ternary system [69]. (**b**) The liquidus projection of the Sn–Bi–Cu ternary system [79]

are the 250°C isothermal section and the liquidus projection [79]. A class I reaction, L = Sn + Bi + ε is at 140.1°C and Sn–54.6wt%Bi–0.014wt%Cu (Sn–40.6at%Bi–0.034at%Cu). Lee et al. [69] predicts the interfacial reaction products between Cu and Sn–58wt%Bi to be the η-Cu_6Sn_5 phase, which is in agreement with the experimental determinations by Vianco et al. [80] and Yoon et al. [81].

Figure 16 is a 300°C phase equilibria isothermal section of the Sn–Bi–Ni system proposed by Lee et al. [82] based on phase diagrams of the three binary constituent systems and very limited phase equilibria measurement. There have been no experimental phase equilibria measurements available except the work of Lee et al. [82]. No ternary compounds have been found and the ternary solubilities of the binary compounds are negligible. Ni_3Sn_2 phase has tie-lines with all the other compounds and the liquid phase. The interfacial reaction product in the Sn–58wt%Bi/Ni couples is the Ni_3Sn_4 phase [81–83]. Lee et al. [82] studied the Sn–Bi/Ni interfacial reactions at 300°C with Sn–Bi alloys of various compositions, and they found that the $NiBi_3$ phase would form when the Bi content was higher than 97.5 wt% (95.7 at%).

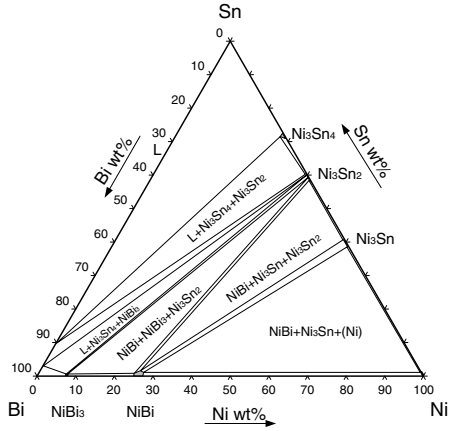

Fig. 16 The 300°C isothermal section of the Sn–Bi–Ni ternary system [82]

5 Sn–Zn–Bi

Sn–Zn–Bi alloys are also possible candidates as Pb-free solders [84–86]. Malakhov et al. [84] carried out thermodynamic assessment and calculated phase diagrams of the Sn–Zn–Bi system. Figure 17a, b are the 170°C isothermal section and liquidus projection, respectively. There are no intermetallic compounds in this system. Both Sn–Zn and Bi–Zn are simple eutectic systems without binary compounds, and the Bi–Zn system has a monotectic and a eutectic reaction [85]. As shown in Fig. 17b, the liquid miscibility gap of the binary Bi–Zn system extends into the ternary system. The class I reaction, liquid = Bi + Sn + Zn, is at 130°C and at Sn–54.54wt%Bi–2.71wt%Zn (Sn–39.39at%Bi–6.25at%Zn). As mentioned previously, the Sn–8wt%Zn–3wt%Bi/Ni couple reacted at 325°C has been examined. Besides the γ-Ni_5Zn_{21} phase, a layer of Sn–35at%Ni–22at%Zn was formed as well [72].

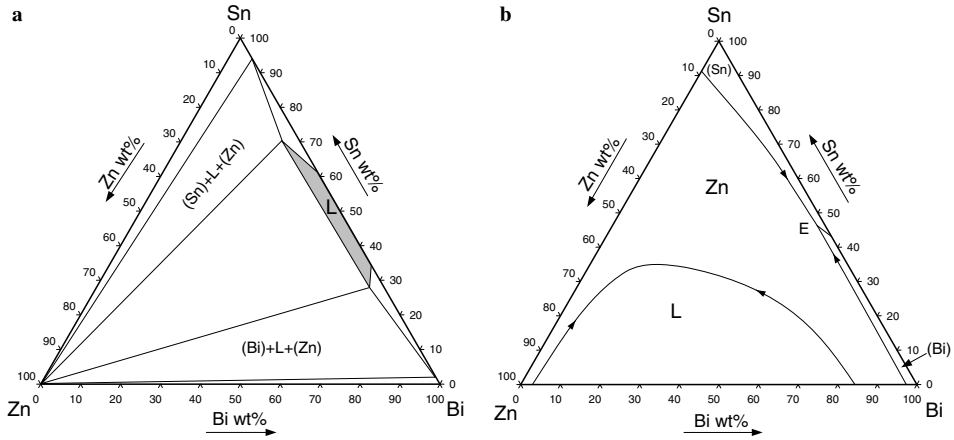

Fig. 17 (**a**) The 170°C isothermal section of the Sn–Bi–Zn ternary system [84]. (**b**) The liquidus projection of the Sn–Bi–Zn ternary system [84]

6 Sn–In

Sn–In alloys have low melting temperatures, high ductility, low substrate dissolution, and good fatigue properties [4, 87–90]. Even though In is expensive, Sn–In alloys are used in various occasions, especially when low soldering temperature is required. Okamoto [91] had a review of the available experimental phase equilibria. Lee et al. thermodynamically modeled the binary Sn–In system and calculated the phase diagram [74]. Figure 18 is the Sn–In binary phase diagram. Both of the intermetallic compounds, β and γ, are with large compositional homogeneity ranges. Solution models were used for the descriptions of these two compounds [74]. The eutectic temperature and composition assessed by Okamoto [91] and Lee et al. [74] are 120°C, Sn–51.7wt%In (Sn–52.5at%In) and 118°C, Sn–52.5at%In, respectively.

Korhonen and Kivilahti [92] and Liu et al. [93] studied the Sn–In–Ag ternary system both experimentally and by thermodynamic modeling. Most recently, Vassilev et al. [94] experimentally determined the Sn–In–Ag equilibrium phase relationship. Isothermal sections at temperatures varied from 113 and 400°C are reported [92–94]. As shown in Fig. 19a of the 180°C isothermal section, no ternary compounds have been

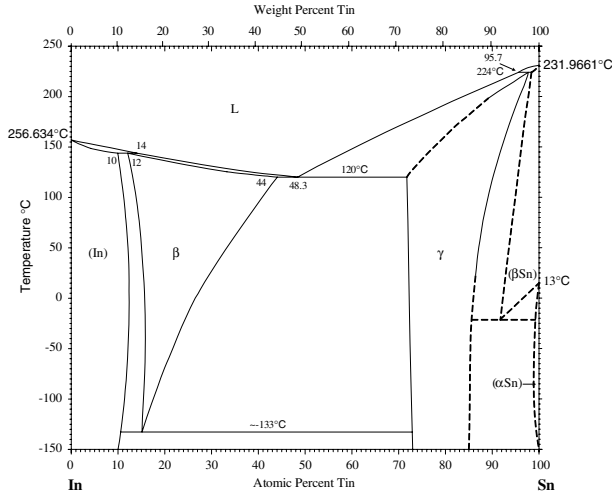

Fig. 18 The Sn–In binary phase diagram [91]

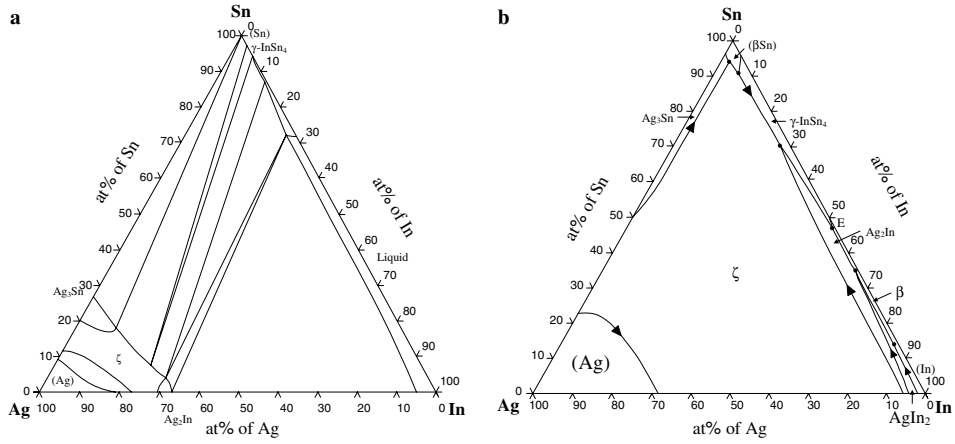

Fig. 19 (**a**) The 180°C isothermal section of the Sn–In–Ag ternary system [93]. (**b**) The liquidus projection of the Sn–In–Ag ternary system [93]

found. A continuous solid solution is formed between the ζ phase in the Ag–Sn and Ag–In systems. However, except for the solid solution, all the other binary compounds do not have significant ternary solubilities. Figure 19b is the calculated liquidus projection. The calculated invariant reaction with the lowest reaction temperature is the class I reaction, liquid = Sn + γ–In-Sn_4 + Ag_2In, at 114°C and Sn–52.2wt%In–0.9wt%Ag (Sn–52.98at%In–0.97at%Ag) [93]. The results are in agreement with experimental determinations. Liu and Chuang [95] and Cheng et al. [96] determined the interfacial reactions between the Sn–In alloys and Ag substrate. In agreement with phase diagram studies, they reported the formation of the Ag_2In and $AgIn_2$ but no ternary compound. Since $AgIn_2$ phase is not stable at most of the reactions temperatures, formation of the $AgIn_2$ phase is likely by precipitation from soldering instead of by interfacial reactions.

Phase diagrams of the Sn–In–Au ternary system has been experimentally determined and assessed [97]. A ternary compound, $Au_4In_3Sn_3$, with Pt_2Sn_3 has been found. Liu et al. [98] developed thermodynamic models to calculate the phase diagrams at 27, 227, 427°C [98]. As shown in Fig. 20 of the calculated 227°C

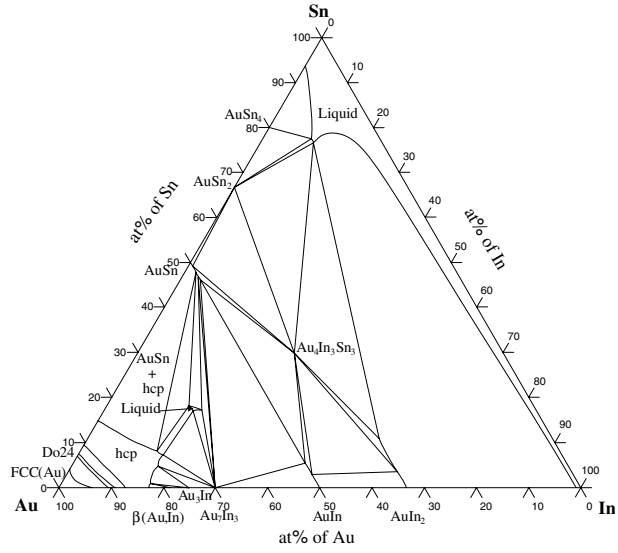

Fig. 20 The 227°C isothermal section of the Sn–In–Au ternary system [98]

isothermal section, two continuous solid solutions are formed at the Au-rich corner, β-$Au_{10}Sn$ and α_1-$Au_{88}In_{12}$ and the ζ phase in Au–In and in Au–Sn systems. Liu et al. [98] also indicated that the $Au_4In_3Sn_3$ was stable in the temperature range from 82 to 428°C, and it melted congruently. Chuang et al. [99] examined the Sn–49wt%In solder ball reactions with the Au/Ni/Cu UBM. They found the interfacial reaction products were $AuIn_2$/AuIn when the temperature was below 170°C, an it transformed into $AuIn_2$ when the temperature was higher than 220°C. The reaction Au–In compounds have significant Ni solubility. Kim and Tu [100] examined the interfacial reactions of 77.2Sn–20In–2.8Ag/Au at 200°C. An $AuIn_2$ type Au_3In_5Sn compound was formed, and after 60 s, the phase decomposed and an Au_2Sn_7In phase was formed. Since both compounds are not found in the Sn–In–Au phase diagrams, they might be meta-stable phases.

Köster et al. [101] determined the phase equilibria of the Sn–In–Cu ternary system at the Cu-rich side, but the phase equilibria close to the In–Sn side which is of primary soldering interests is lacking. At 400°C, two ternary compounds and a continuous solid solution formed between the η-Cu_2In and the η-Cu_6Sn_5 phases are observed. Liu et al. [102] determined the phase equilibria of the Sn–In–Cu system both by thermodynamic calculation and experimental determination. They have found only one ternary compound, $Cu_{16}In_3Sn$ at higher temperature, and a ternary compound Cu_2In_3Sn at 110°C. Liu et al. [102] also calculated the isothermal sections at various temperatures using thermodynamic models developed by them. Lin et al. [103] experimentally determined the phase diagrams. Figure 21a is the 250°C isothermal section of the Sn–In–Cu system [103]. They confirmed the formation of the continuous solid solutions; however, they do not observe the formation of ternary compounds. Significant solubilities are found for the ε-Cu_3Sn with In and for the Cu_7In_3 with Sn. Figure 21b is its liquidus projection determined by Lin et al. [103]. The result is similar to that calculated by Liu et al. [102]. However, the Sn–Cu phase diagram calculated by Liu et al. is different from those by Shim et al. [12] and Boettinger et al. [13]. The Sn–Cu phase diagram by Liu et al. does not have the peritectic reaction, liquid + β = γ, thus the liquidus trough originated from this binary peritectic is missing in the Sn–In–Cu liquidus projection proposed by Liu et al.[102].

Romig et al. [104] studied the interfacial reactions of the Sn–50wt%In/Cu couples at 70 and 90°C, and $Cu_2(Sn,In)$ and Cu_2In_3Sn were found. Vianco et al. [105] examined the Sn–50wt%In/Cu couples at temperatures varied from 55 to 100°C, and they found the formation of $Cu_{26}Sn_{13}In_8$ and $Cu_{17}Sn_9In_{24}$. It is presumed these two phases are the η-Cu_6Sn_5 with high In solubilities, and $CuIn_2$ with high Sn solubility. Chuang et al. [106] studied the Sn–51wt%In/Cu couple at 150–400°C, and they found ε-$Cu_3(In,Sn)$ and η-$Cu_6(In,Sn)_5$. Sommadossi et al. [107] studied the interfacial reactions of the Sn–52at%In/Cu couples. They found the formation of η-Cu_3Sn at 180°C, and ε-Cu_3Sn and η-Cu_6Sn_5 at 290°C. The compositions of these phases are Sn–27at%In–57at%Cu and Sn–10at%In–77at%Cu, respectively. Kim and Jung [108] studied the Sn–52at%In/Cu interfacial reactions at 70–100°C, and they found the formation of the $Cu(In,Sn)_2$

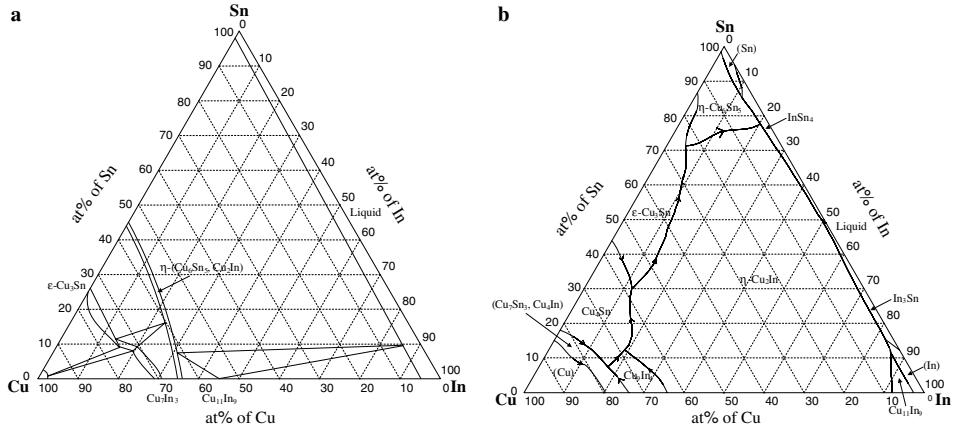

Fig. 21 (**a**) The 250°C isothermal section of the Sn–In–Cu ternary system [103]. (**b**) The liquidus projection of the Sn–In–Cu ternary system [103]

and $Cu_6(In,Sn)_5$ phases. The reaction products can be well interpreted with the isothermal section as shown in Fig. 21a except for the $CuIn_2$ phase. The $CuIn_2$ phase is likely a metastable phase since it is not found in the binary Cu–In system either [102].

Burkhardt and Schubert [109], Bhargava and Schubert [110], and Shadangi et al. [111] determined the phase relationship of the Sn–In–Ni ternary system at higher temperature and at the Ni-rich corner. Burkhardt and Schubert [109] reported a continuous solid solution formed by Ni_3Sn and Ni_3In. Bhargava and Schubert [110] indicated the existence of the ternary compound Ni_6InSn_5, and one more solid solution formed by Ni_3In_2 and Ni_3Sn_2. Huang and Chen [112] examined the phase diagram at lower temperature at 240°C. As shown in Fig. 22 of the 240°C Sn–In–Ni isothermal section, they found the continuous solid solution between Ni_3In and Ni_3Sn. They also found most of the binary compounds have significant solubilities but did not find the ternary compound. Huang and Chen [112] examined the Sn–In/Ni interfacial reactions at 160 and 240°C, and they found Ni_3Sn_4 is the primary reaction products and the $Ni_{28}In_{72}$ phase is formed only in the couples prepared with In-rich alloys. Kim and Jung [113] examined the intermetallic compound layer growth between In and Sn–52at%In with Ni/Cu substrate at 70–120°C. They found the formation of $In_{27}Ni_{10}$ and $Ni_3(In,Sn)_4$ for indium and the Sn–In alloy, respectively. The very extensive solubility found in the Ni_3Sn_4 phase by Kim and Jung [112] is in agreement with the phase diagram determination [112]. Chuang et al. [114] studied the interfacial reactions between the Sn–20wt%In–2.8wt%Ag with Ni substrate, and they also found the formation of Ni_3Sn_4 phase. However, no significant In solubility in the Ni_3Sn_4 phase was found.

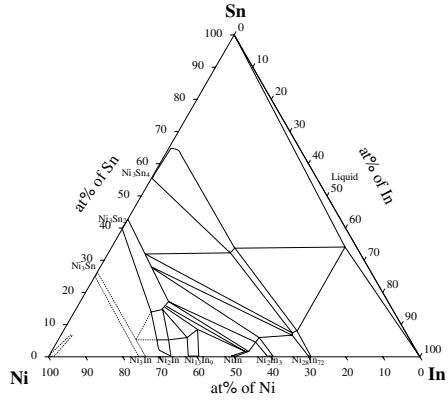

Fig. 22 The 240°C isothermal section of the Sn–In–Ni ternary system [112]

7 Sn–Sb

Because of the requirements of step soldering, solders of different melting points are needed. Although there are very intensive studies of Pb-free solders for replacing the low-melting-point eutectic Sn–Pb, very few efforts are found for the replacement of high temperature Sn–95wt%Pb and Sn–90wt%Pb solders. Sn–Sb and Sn–Sb based alloys are promising Pb-free solders. This is especially true of Sn–5wt%Sb (Sn–4.53at%Sb), which is used as high temperature solder [115–117].

Predel and Schwermann [118] carried out phase equilibria study of the Sn–Sb system, and proposed the diagram as shown in Fig. 23 based on their experimental determinations and the phase equilibria results in the literatures. There are three peritectic and one eutectoid reactions. The temperature of the peritectic reaction at the Sn side, liquid + Sn_3Sb_2 = Sn, is at 250°C. The Sn_3Sb_2 compound has negligible compositional homogeneity and is stable only in a short temperature range between 242°C and 324°C. Jonsson and Agren [119] analyzed the experimental thermodynamic and phase equilibria data and developed thermodynamic models. The intermetallic β phase has large compositional homogeneity range and is described by using two-sublattices models. The Sn_3Sb_2 is treated as a line compound. The calculated Sn–Sb phase diagram using the developed models is in good agreement with the experimental determinations as shown in Fig. 23.

Oh et al. [120] and Moser et al. [121] thermodynamically assessed the ternary Sn–Sb–Ag system, and calculated the isothermal sections, isoplethal sections, and liquidus projection. Figure 24a is the calculated 100°C isothermal section of the Sn–Sb–Ag phase equilibria [121]. No ternary compounds have been found. Two continuous solid solutions are formed, and they are the ζ-$Ag_4(Sb,Sn)$ and the ε-$Ag_3(Sb,Sn)$. Figure 24b is the calculated liquidus projection. The calculation result is in agreement with the experimentally determined liquidus projection by Masson and Kirkpatrick [122]. The invariant reaction at the Sn corner with the lowest reaction temperature is a class II reaction, liquid + Sn_3Sb_2 = ε-$Ag_3(Sb,Sn)$ + Sn. The reaction temperatures and composition of the liquid are 235°C and Sn–6at%Sb–5at%Sb and 231.5°C and Sn–6.2at%Sb–3.4at%Sb as calculated by Oh et al. [120] and Moser et al. [121], respectively.

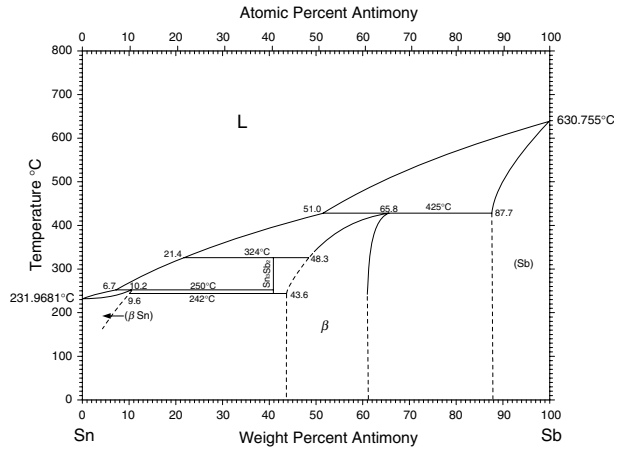

Fig. 23 The Sn–Sb binary phase diagram [118]

A thermodynamic assessment of the Sn–Sb–Au ternary system was conducted by Kim et al. [123] and they also calculated its isothermal sections, isoplethal sections and liquidus projection. Figure 25a, b are the isothermal section at 200°C and the liquid projection, respectively. No ternary compounds have been observed. The $AuSb_2$ is with about 15at%Sn solubility; however, the Sb solubility in $AuSn_2$ is negligible. As shown in Fig. 25b, the invariant reaction at the Sn-rich corner with the lowest reaction temperature is a class II reaction, liquid + Sb_2Sn_3 = Sn + $AuSn_4$ at 491°C.

There are no phase equilibria studies of the Sn–Sb–Cu system. Jang et al. [116] and Takaku et al. [124] examined interfacial reactions of the Sn–Sb solders on Cu substrates. They found the formation of ε-Cu_3Sn and η-Cu_6Sn_5 phases. Jang et al. [116] also found the formation of Sn_3Sb_2 phase in the Sn–15wt%Sb (Sn–14.68at%Sb) couples. No ternary compounds were reported in both studies [116, 124]. Available phase diagrams of the Sn–Sb–Ni ternary system are all at the Ni-rich corner and their temperatures are at 450°C and 500°C [125]. No phase equilibria information of the Sn–Sb–Ni ternary system is at the temperature and compositional ranges of soldering interests, and no interfacial reactions studies of the Sn–Sb/Ni have been found either.

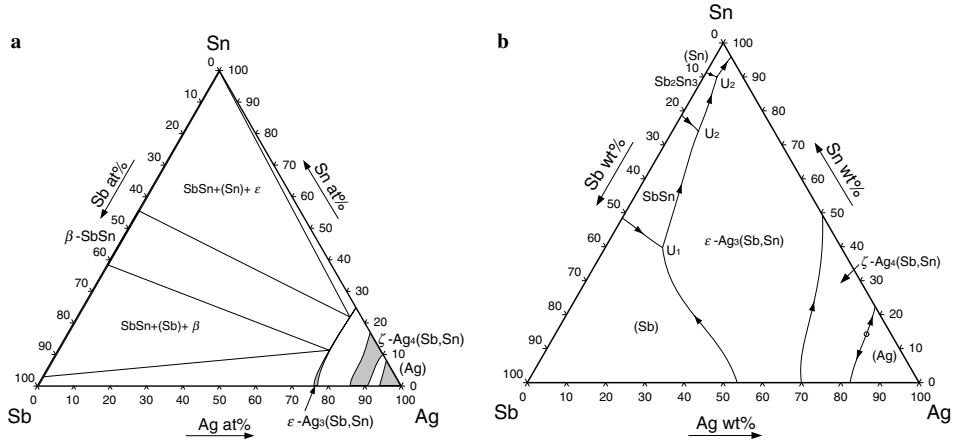

Fig. 24 (**a**) The 100°C isothermal section of the Sn–Sb–Ag ternary system [121]. (**b**) The liquidus projection of the Sn–Sb–Ag ternary system [121]

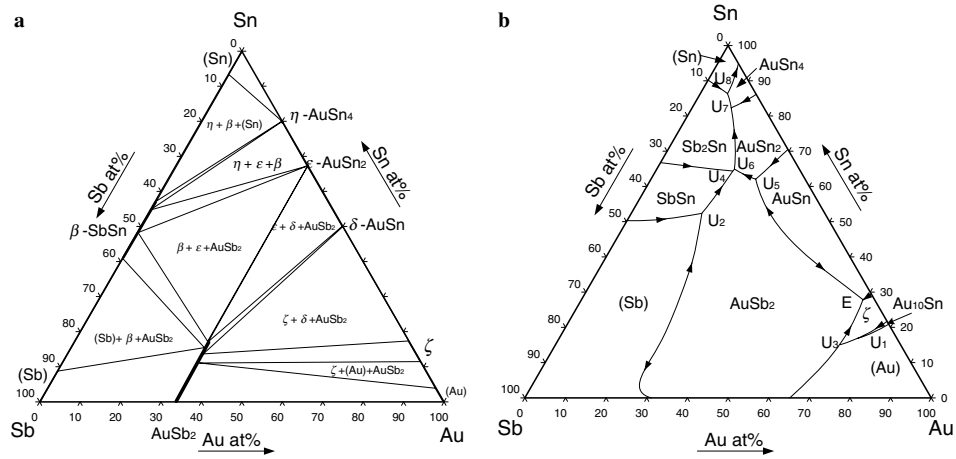

Fig. 25 (**a**) The 200°C isothermal section of the Sn–Sb–Au ternary system [123]. (**b**) The liquidus projection of the Sn–Sb–Au ternary system [123]

8 Conclusions

Phase diagrams are the roadmaps for the exploration of materials technology. Bird's-eye views of the phase diagrams of Pb-free solders and their related materials systems are mostly available. However, complete and accurate phase diagrams are lacking for almost all the ternary and quaternary systems. Experimental determinations of the multi-component phase diagrams over the entire compositional and temperature ranges of soldering interests are extremely difficult if not impossible. The CALPHAD approach which combines thermodynamic models of constituent binary systems and limited phase equilibria data of ternary and quaternary systems is suitable for the phase diagram determinations of higher order materials systems, but the calculated phase diagrams cannot be accurate without the input of reliable experimental values at some critical points. Only after the first-step calculation, the critical points can be pointed out and experimental efforts can be carried out with focus. Close cooperation and interaction between phase diagram calculation and experimental determination are crucial for the determinations of Pb-free solders and their related materials systems.

Acknowledgement The authors acknowledge the financial support of National Science Council. (NSC94-2214-E-007-006).

References

1. R.J. Klein Wassink, in *Soldering in Electronics*, 2nd edn. (Electrochemical Publications, Isle of Man, 1989)
2. Official Journal of the European Union, p. L 37/19-L 37/23, 13.2.2003
3. J. Bath, C. Handwerker, E. Bradley, Circ. Assembly **5**, 31 (2000)
4. M. Abtew, G. Selvaduray, Mater. Sci. Eng. R **27**, 95 (2000)
5. T. Laurila, V. Vuorinen, J.K. Kivilahti, Mater. Sci. Eng. R **49**, 1 (2005)
6. D.R. Frear, W.B. Jones, K.R. Kinsman, in *Solder Mechanics: A State of the Art Assessment* (Minerals, Metals & Materials Society, Warrendale, Pa, 1991)
7. ''Roadmap 2002 for Commercialization of Lead-free Solder'', Lead-Free Soldering Roadmap Committee, Japan Electronics and Information Technology industries Association (JEITA) (2002)
8. ''Lead-free Assembly Projects'', National Electronics Manufacturing Initiatives(NEMI) (1999)
9. I. Karakaya, W.T. Thompson, Bull. Alloy Phase Diagrams **8**, 340 (1987)
10. U.R. Kattner, W.J. Boettinger, J. Electron. Mater. **23**, 603 (1994)
11. N. Saunders, A.P. Miodownik, Bull. Alloy Phase Diagrams **11**, 278 (1990)
12. J.H. Shim, C.S. Oh, B.J. Lee, D.N. Lee, Z. Metallkd. **87**, 205 (1996)
13. W.J. Boettinger, C.A. Handwerker, U.R. Kattner, in *The Mechanics of Solder Alloy Wetting and Spreading* (Van Nostrand Reinhold, New York, 1993), p. 103
14. E. Gebhardt, G. Petzow, Z. Metallkd. **50**, 597 (1959)
15. Y.W. Yen, S.-W. Chen, J. Mater. Res. **19**, 2298 (2004)
16. C.M. Miller, I.E. Anderson, J.F. Smith, J. Electron. Mater. **23**, 595 (1994)
17. M.E. Loomans, M.E. Fine, Metall. Trans. A **31**, 1155 (2000)
18. K.W. Moon, W.J. Boettinger, U.R. Kattner, F.S. Biancaniello, C.A. Handwereker, J. Electron. Mater. **29**, 1122 (2000)
19. I. Ohnuma, M. Miyashita, K. Anzai, X.J. Liu, H. Ohtani, R. Kainuma, K. Ishida, J. Electron. Mater. **29**, 1137 (2000)
20. T.B. Massalski, H. Pops, Acta Metall. **18**, 961 (1970)
21. D.S. Evans, A. Prince, Met. Sci. **8**, 286 (1974)
22. S.-W. Chen, Y.W. Yen, J. Electron. Mater. **30**, 1133 (2001)
23. J. London, D.W. Ashall, Brazing Solder. **11**, 49 (1986)

24. P.T. Vianco, K.L. Erickson, P.L. Hopkins, J. Electron. Mater. **23**, 721 (1994)
25. S.-W. Chen, Y.W. Yen, J. Electron. Mater. **28**, 1203 (1999)
26. S. Choi, T.R. Bieler, J.P. Lucas, K.N. Subramanian, J. Electron. Mater. **28**, 1209 (1999)
27. T.Y. Lee, W.J. Choi, K.N. Tu, J.W. Jang, S.M. Kuo, J.K. Lin, D.R. Frear, K. Zeng, J.K. Kivilahti, J. Mater. Res. **17**, 291 (2002)
28. H.F. Hsu, S.-W. Chen, Acta Mater. **52**, 2541 (2004)
29. S.-W. Chen, H.F. Hsu, C.W. Lin, J. Mater. Res. **19**, 2262 (2004)
30. H.D. Blair, T.Y. Pan, J.M. Nicholson, in *Proceedings of the 48th Electronic Components and Technology Conference*, 1998 p. 259
31. C.M. Chen, S.-W. Chen, J. Appl. Phys. **90**, 1208 (2001)
32. C.E. Ho, R.Y. Tsai, Y.L. Lin, C.R. Kao, J. Electron. Mater. **31**, 584 (2002)
33. C.C. Chen, S.-W. Chen, C.Y. Kao, J. Electron. Mater. **35**, 922 (2006)
34. O.B. Karlsen, A. Kjekshus, E. Roest, Acta Chem. Scand. **46**, 147 (1992)
35. B. Peplinski, E. Zakel, Mater. Sci. Forum **166–169**, 443 (1994)
36. C.N.C. Luciano, K.I. Udoh, M. Nakagawa, S. Matsuya, M. Ohta, J. Alloys Comp. **337**, 289 (2002)
37. C.E. Ho, Y.M. Chen, C.R. Kao, J. Electron. Mater. **28**, 1231 (1999)
38. C.H. Lin, S.-W. Chen, C.H. Wang, J. Electron. Mater. **31**, 907 (2002)
39. C.H. Wang, S.-W. Chen, Metall. Trans. A **34**, 2281 (2003)
40. S.-W. Chen, S.H. Wu, S.W. Lee, J. Electron. Mater. **32**, 1188 (2003)
41. Y. Murakami, S. Kachi, Trans. JIM. **24**, 9 (1983)
42. P. Oberndorff, PhD Thesis, Technical University of Eindhoven, Eindhoven, Nerthelands (2001)
43. J. Miettinen, CALPHAD **27**, 309 (2003)
44. J.K. Lin, A. De Silva, D. Frear, Y. Guo, J.W. Jang, L. Li, D. Mitchell, B. Yeung, C. Zhang, in *Proceedings of the 51st Electronic Components and Technology Conference*, 2001 p. 455
45. W.T. Chen, C.E. Ho, C.R. Kao, J. Mater. Res. **17**, 263 (2002)
46. S.-W. Chen, S.W. Lee, M.C. Yip, J. Electron. Mater. **32**, 1284 (2003)
47. C.H. Wang, S.-W. Chen, Acta Mater. **54**, 247 (2006)
48. S.-W. Chen, C.A. Chang, J. Electron. Mater. **33**, 1071 (2004)
49. C.A. Chang, S.-W. Chen, C.N. Chiu, Y.C. Huang, J. Electron. Mater. **34**, 1135 (2005)
50. C.N. Chiu, Y.C. Huang, A.R. Zi, S.-W. Chen, Mater. Trans. **46**, 2426 (2005)
51. A. Zribi, A. Clark, L. Zavalij, P. Borgesen, E.J. Cotts, J. Electron. Mater. **30**, 1157 (2001)
52. K. Zeng, V. Vuorinen, J.K. Kivilahti, IEEE Trans. Electron. Packag. Manufact. **25**, 162 (2002)
53. K.S. Kim, S.H. Huh, K. Suganuma, J. Alloys Comp. **352**, 226 (2003)
54. M.D. Cheng, S.Y. Chang, S.F. Yen, T.H. Chuang, J. Electron. Mater. **33**, 171 (2004)
55. W.C. Luo, C.E. Ho, J.Y. Tsai, Y.L. Lin, C.R. Kao, Mater. Sci. Eng. A **396**, 385 (2005)
56. U.R. Kattner, JOM **49**(12), 14 (1997)
57. H.T. Luo, S.-W. Chen, J. Mater. Sci. **31**, 5059 (1996)
58. Z. Moser, J. Dutkiewicz, W. Gasior, J. Salawa, Bull. Alloy Phase Diagrams **4**, 330 (1985)
59. K. Suganuma, K. Niihara, T. Shoutoku, Y. Nakamura, J. Mater. Res. **13**, 2859 (1998)
60. K.-L. Lin, T.-P. Liu, Oxid. Met. **50**, 255 (1998)
61. Y.C. Chan, M.Y. Chiu, T.H. Chuang, Z. Metallkd. **93**, 95 (2002)
62. I. Shohji, T. Nakamura, F. Mori, S. Fujiuchi, Mater. Trans. **43**, 1797 (2002)
63. J.-M. Song, K.-L. Lin, J. Mater. Res. **18**, 2060 (2003)
64. K.-S. Kim, J.-M. Yang, C.-H. Yu, I.-O. Jung, H.-H. Kim, J. Alloys Compd. **379**, 314 (2004)
65. M. Date, K.N. Tu, T. Shoji, M. Fujiyoshi, K. Sato, J. Mater. Res. **19**, 2887 (2004)
66. C.-W. Huang, K.-L. Lin, J. Mater. Res. **19**, 3560 (2004)
67. B.-J. Lee, CALPHAD **20**, 471 (1996)
68. H. Ohtani, M. Miyashita, K. Ishida, J. Jpn. Inst. Met. **63**, 685 (1999)
69. B.-J. Lee, N.M. Hwang, H.M. Lee, Acta Mater. **45**, 1867 (1997)
70. C.-Y. Chou, S.-W. Chen, Acta Mater. **54**, 2393 (2006)
71. C.-Y. Chou, S.-W. Chen, Y. S. Chang, J. Mater. Res. **21**, 1849 (2006)
72. M.Y. Chiu, S.S. Wang, T.H. Chuang, J. Electron. Mater. **31**, 494 (2002)
73. H. Okamoto, in *Binary Alloy Phase Diagram*, 2nd edn. (ASM, Metals Park, Ohio, 1990), p. 794
74. B.-J. Lee, C.-S. Oh, J.-H. Shim, J. Electron. Mater. **25**, 983 (1996)
75. S. Hassam, E. Dichi, B. Legendre, J. Alloys Compd. **268**, 199 (1998)
76. H. Ohtani, I. Satoh, M. Miyashita, K. Ishida, Mater. Trans. **42**, 722 (2001)
77. A. Prince, G.V. Raynor, D.S. Evans, in *Phase Diagrams of Ternary Gold Alloys* (Institute of Metals, London, 1990) p. 168
78. D. Kim, C.C. Lee, in *Proceedings of the 53rd Electronic Components and Technology Conference*, New Orleans, USA, May 2003, p. 668
79. K. Doi, H. Ohtani, M. Hasebe, Mater. Trans. **45**, 380 (2004)
80. P.T. Vianco, A.C. Kilgo, R. Grant, J. Electron. Mater. **24**, 1493 (1995)
81. J.-W. Yoon, C.-B. Lee, S.-B. Jung, Mater. Trans. **43**, 1821 (2002)
82. J.-I. Lee, S.-W. Chen, H.-Y. Chang, C.-M. Chen, J. Electron. Mater. **32**, 117 (2003)
83. W.H. Tao, C. Chen, C.E. Ho, W.T. Chen, C.R. Kao, Chem. Mater. **13**, 1051 (2001)
84. D.V. Malakhov, X.J. Liu, I. Ohnuma, K. Ishida, J. Phase Equilib. **21**, 514 (2000)
85. H. Paul, Solder. Surf. Mount Technol. **11**, 46 (1999)
86. N. Moelans, K.C. Hari, P. Wollants, J. Alloys Compd. **360**, 98 (2003)
87. Z. Mei, J.W. Morris Jr., J. Electron. Mater. **21**, 401 (1992)
88. K. Shimizu, T. Nakanishi, K. Karasawa, K. Hashimoto, K. Niwa, J. Electron. Mater. **24**, 39 (1995)
89. N.C. Lee, Solder. Surf. Mount Technol. **9**, 65 (1997)
90. A.T. Kosilov, G.L. Polner, I.U. Smurov, V.V. Zenin, Sci. Technol. Weld. Joining **9**, 169 (2004)
91. H. Okamoto, in *Phase Diagrams of Indium Alloys and Their Engineering Application*, ed. by C.E.T. White, H. Okamoto (ASM international, Materials Park, OH, 1992), pp. 255–257
92. T.M. Korhonen, J.K. Kivilahti, J. Electron. Mater. **27**, 149 (1998)
93. X.J. Liu, Y. Inohana, Y. Takaku, I. Ohnuma, R. Kainuma, K. Ishida, Z. Moser, W. Gasior, J. Pstrus, J. Electron. Mater. **31**, 1139 (2002)
94. G.P. Vassilev, E.S. Dobrev, J.-C. Tedenac, J. Alloys Compd. **399**, 118 (2005)

95. Y.M. Liu, T.H. Chuang, J. Electron. Mater. **29**, 1328 (2000)
96. M.D. Cheng, S.S. Wang, T.H. Chuang, J. Electron. Mater. **31**, 171 (2002)
97. A. Prince, G.V. Raynor, D.S. Evans, in *Phase Diagrams of Ternary Gold Alloys*, ed. by A. Prince, V. Raynor, D.S. Evans (The Institute of Metals, London, 1990), pp. 300–302
98. H.S. Liu, C. Liu, K. Ishida, Z.P. Jin, J. Electron. Mater. **32**, 1290 (2003)
99. T.H. Chuang, S.Y. Chang, L.C. Tsao, W.P. Weng, H.M. Wu, J. Electron. Mater. **32**, 195 (2003)
100. P.G. Kim, K.N. Tu, Mater. Chem. Phys. **53**, 165 (1998)
101. W. Köster, T. Gödecke, D. Heine, Z. Metallkd. Bd. 63, H. 12 (1972) 802
102. X.J. Liu, H.S. Liu, I. Ohnuma, R. Kainuma, K. Ishida, S. Itabashi, K. Kameda, K. Yamaguchi, J. Electron. Mater. **30**, 1093 (2001)
103. S.-K. Lin, T.-Y. Chung, S.-W. Chen, Y.-W. Yen, unpublished results, (2006)
104. A.D. Romig Jr., F.G. Yost, P.F. Hlava, in *Microbeam Analysis-1984* ed. by A.D. Romig Jr., J.I. Goldstein (San Francisco Press, 1984), p. 87
105. P.T. Vianco, P.F. Hlava, A.C. Kilgo, J. Electron. Mater. **23**, 583 (1994)
106. T.H. Chuang, C.L. Yu, S.Y. Chang, S.S. Wang, J. Electron. Mater. **31**, 640 (2002)
107. S. Sommadossi, W. Gust, E.J. Mitteneijer, Mater. Chem. Phys. **77**, 924 (2003)
108. D.-G. Kim, S.-B. Jung, J. Alloys Compd. **386**, 1515 (2005)
109. W. Burkhardt, K. Schubert, Z. Metallkd **50**, 442 (1959)
110. M.K. Bhargava, K. Schubert, Z. Metallkd. **67**, 318 (1976)
111. S.K. Shadangi, M. Singh, S.C. Panda, S. Bhan, Indian J. Technol. **24**, 105 (1986)
112. C.-Y. Huang, S.-W. Chen, J. Electron. Mater. **31**, 152 (2002)
113. D.-G. Kim, S.-B. Jung, J. Electron. Mater. **33**, 1561 (2004)
114. T.H. Chuang, K.W. Huang, W.H. Lin, J. Electron. Mater. **33**, 374 (2004)
115. R.K. Mahidhara, S.M.L. Sastry, I. Turlik, K.K. Murty, Scripta Metall. Mater. **31**, 1145 (1994)
116. J.W. Jang, P.G. Kim, K.N. Tu, M. Lee, J. Mater. Res. **14**, 3895 (1999)
117. A.R. Geranmayeh, R. Mahmudi, J. Mater. Sci. **40**, 3361 (2005)
118. B. Predel, W. Schwermann, J. Inst. Met. **99**, 169 (1971)
119. B. Jonsson, J. Agren, Mater. Sci. Technol. **2**, 913 (1986)
120. C.-S. Oh, J.-H. Shim, B.-J. Lee, D.N. Lee, J. Alloys Compd. **238**, 155 (1996)
121. Z. Moser, W. Gasior, J. Pstrus, S. Ishihara, X.J. Liu, I. Ohnuma, R. Kainuma, K. Ishida, Mater. Trans. **45**, 652 (2004)
122. D.B. Masson, B.K. Kirkpatrick, J. Electro. Mater. **15**, 349 (1986)
123. J.H. Kim, S.W. Jeong, H.M. Lee, J. Electron. Mater. **31**, 557 (2002)
124. Y. Takaku, X.J. Liu, I. Ohnuma, R. Kainuma, K. Ishida, Mater. Trans. **45**, 646 (2004)
125. P. Villars, A. Prince, H. Okamoto, in *Handbook of Ternary Alloy Phase Diagram* (ASM, Metals Park, Ohio, 1995), p. 13010